Dynamics of an Arbitrary Flexible Body in Large Rotation and Translation

Arun K. Banerjee* and John M. Dickens†
Lockheed Missiles & Space Company, Sunnyvale, California 94086

Conventional theories underlying many multibody codes used for simulating the behavior of elastic structures undergoing large rotation and translation with small vibrations fail to predict dynamic stiffening of the structures. This can lead to significantly incorrect simulations in many practical situations. A theory that does not suffer from this defect and is valid for an *arbitrary* structure is given here. The formulation is based on Kane's equations and consists of two steps: First, generalized inertia forces are written for an arbitrary structure for which one is forced to linearize prematurely in the modal coordinates; next, this defect in linearization is compensated for by the introduction of contributions to the generalized active forces from the "motion stiffness" of the structure. The stress associated with the motion stiffness is identified as due to 12 sets of inertia forces and 9 sets of inertia couples distributed throughout the body during the most general motion of its flying reference frame. An algorithm is set for a reader wishing to implement the theory, and illustrative examples are given to demonstrate the validity and generality of the formulation.

I. Introduction

CORRECT predictions of the behavior of flexible bodies undergoing motions that can be described, loosely speaking, as large rigid-body rotations and translations accompanied by small elastic vibrations is a subject of major concern in the aerospace industry. Hence, one might imagine that a sound theory for simulating such motions has long been in hand. That this is not so was pointed out by Kane et al.,[1] who presented a theory for beams in large overall motion, and showed that erroneous results, such as prediction of dynamic softening of a rotating structure when dynamic stiffening is to be expected, could be obtained in many cases of practical interest with conventional theories underlying certain publicly available simulation codes. This was recognized as a major issue at a multibody dynamics conference (Ref. 2) conducted by NASA's Jet Propulsion Laboratory in October 1987.

The formulation errors in the conventional formalisms exist because the underlying derivations contain terms in which linearizations have been performed prematurely in the modal coordinates. When this linearization is performed properly, that is, in a manner consistent with the constraints of deformation of a structure, then all is well, as was shown for beams in Ref. 1, and for plates by Banerjee and Kane.[3] Unfortunately, for an *arbitrary* structure, there is no general way to express the deformation constraints. Consequently, use of vibration modes, which always display a lack of interdependence between the elastic displacement components, thus forces one to perform a premature linearization, and this leads to a fundamentally flawed formulation.

The phenomenon of spin stiffening of rotating beams has long been known and is treated, for example, in the texts by Bisplinghoff et al.[4] and Meirovitch.[5] For more general rotating structures, Likins[6] suggested the use of geometric stiffness augmenting the structural stiffness in order to correctly represent the dynamic response. Levinson and Kane[7] incorporated geometric stiffness of beams in their finite-element-based analysis of spinning spacecraft with radial booms. In the field of mechanisms, a nonlinear geometric finite-element method was proposed, and simulations were validated by experiments by Turcic and Midha[8] and Turcic et al.[9] More recently, exact theories for large overall motion of continua, including large elastic deformations, have been developed by Simo and Vu-Quoc,[10,11] and their solution procedure is also based on the (nonlinear) finite-element method. Finite-element theory, with its power and versatility, has been applied to the dynamics of articulated structures with notable success by Housner et al.,[12] but the large number of nodal variables needed to represent multibody structures of practical size and complexity makes the approach computationally unwieldy. Therefore, theories that achieve model reduction through the use of vibration modes, yet capture correctly the phenomenon of dynamic stiffening (softening), are highly desirable. Wu and Haug[13] accomplish this by dividing a single flexible body into substructures and constraining the relative motion between the substructures at common nodes, much like Hopkins and Likins[14] had done earlier for rotating structures, except that they represent the substructure with modes rather than as finite elements; their formulation thus requires the solution for modal coordinates of each substructure and the constraint forces and moments at the interface nodes. Representation of dynamic stiffening through direct use of geometric stiffness has been made for general structures by Modi and Ibrahim[15] and Zeiler and Buttrill,[16] and for beams by Amirouche and Ider.[17] However, the implementation of geometric stiffness in these formulations, based on the instantaneous nodal displacements, seems to be computationally intensive, even with the use of modes.

In this paper, we introduce the idea of "motion stiffness," or stiffness associated with the most general motion of the reference frame for the elastic body, by recognizing such stiffness as a form of geometric stiffness caused by a system of 12 inertia forces and 9 inertia couples distributed throughout the body. We show that a consideration of this motion stiffness compensates for the unavoidable errors caused by the premature linearization process for an arbitrary, elastic structure whose motion is characterized by vibration modes in a reference frame undergoing large rotation and translation.

The power of the new formulation becomes apparent in connection with an example of an arbitrary flexible body for which there does not exist a theory, so far as we know, that

Received Aug. 16, 1988; revision received Nov. 30, 1988; presented as Paper 89-1308 at the AIAA/ASME/ASCE/AHS Structures, Structural Dynamics, and Materials Conference, Mobile, AL, April 3-5, 1989.

*Senior Staff Engineer, Structural Dynamics.
†Staff Engineer, Structural Dynamics.

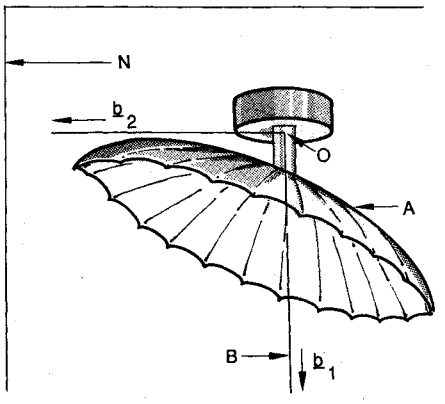

Fig. 1 Dual-spin spacecraft with flexible, spinning offset paraboloidal antenna.

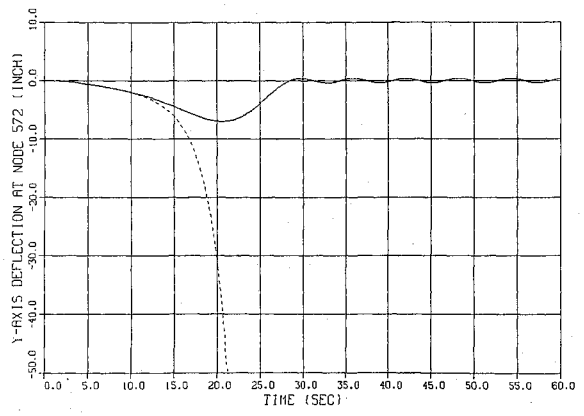

Fig. 2 Elastic displacement along y axis at a finite-element node of paraboloidal antenna for spin-up given by present theory (solid line) and a conventional theory (dashed line); steady-state spin frequency is greater than the first mode vibration frequency.

captures dynamic stiffening, using modes and without substructuring. Figure 1 shows a dual-spin spacecraft that has an Earth-pointing, spinning, offset paraboloidal antenna represented in a finite-element model by an assemblage of rods, beams, membranes, and rigid mass inclusions. (The values of the moduli of elasticity for the materials of the model were uniformly reduced from those for an actual spacecraft to produce a first-mode frequency lower than the spin frequency; this will facilitate the making of our point regarding the capture of dynamic stiffening of an arbitrary structure characterized by its vibration modes.) Suppose that the antenna A is rigidly attached to a reference frame B at O; B is subjected to a spin-up maneuver such that the spin-axis vector $\boldsymbol{b}_1$ remains fixed in a Newtonian reference frame N, and ω_1, the component of the angular velocity of B in N along $\boldsymbol{b}_1$, measured in radians per second, is given by

$$\omega_1 = \frac{\Omega}{T}\left(t - \frac{T}{2\pi}\sin\frac{2\pi t}{T}\right), \qquad t < T$$
$$= \Omega, \qquad t > T \tag{1}$$

where Ω is the steady-state spin speed in radians per second, and T is the spin-up time in seconds. The solid curve in Fig. 2 shows the elastic displacement along $\boldsymbol{b}_2$ of node number 572 of the finite-element model, a point located by the coordinates (255.6, 0.0, −89.0) in inch units in the B frame for the undeformed configuration, as given by the present theory, for

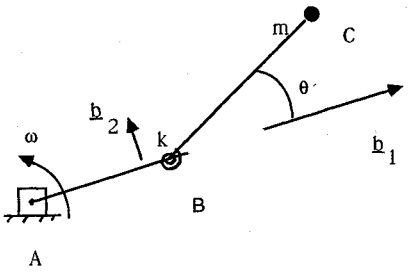

Fig. 3 A simple mechanical system for studying dynamic stiffening with rotational motion.

spin-up with $\Omega = \pi$ (or 0.5 Hz), $T = 30.0$, where Ω exceeds the fundamental natural frequency of vibration of the structure, 0.433 Hz. We will presently see that this response is a typical signature of a system undergoing dynamic stiffening during a spin-up motion. To emphasize the significance of the present theory, we have also plotted in Fig. 2 a dashed curve that is given by a conventional theory (Refs. 18 and 19) and is obtained here by deleting the inertia stiffness terms of our theory. Note that the conventional theory predicts unbounded motion of node 572, clearly an erroneous result.

To aid in the presentation of the theory that produced the solid curve in Fig. 2, we first consider in Sec. II a simple example that established the essential ideas. The general theory is then presented for a single flexible body in Secs. III and IV, and an algorithm is presented in Sec. V. Additional simulation results validating the theory by comparisons with previously published results obtained with special-purpose theories for beams and plates are given in Sec. VI, followed by discussions on the scope of the formulation.

II. Simple Example

The following example, suggested to us by Thomas R. Kane of Stanford University, serves to illustrate the essence of the problem and the solution. Referring to Fig. 3, consider two massless rigid rods AB and BC connected at the hinge B by a torsional spring of stiffness k. Rod AB of length R is driven by a motor at the angular speed $\omega(t)$. Rod BC of length L has a particle of mass m attached at C. The angle $\theta(t)$ between AB and BC is initially zero and is assumed to remain small during the motion. Linearizing prematurely in the angle, one can write the velocity of C in terms of the unit vectors fixed in AB (see Fig. 3) as

$$v = -\omega L\theta \boldsymbol{b}_1 + [\omega(R + L) + L\dot{\theta}]\boldsymbol{b}_2 \tag{2}$$

Forming the kinetic energy expression with Eq. (2), considering the potential energy due to the spring k, and substituting these in Lagrange's equation, one gets the equation

$$mL^2\ddot{\theta} + (k - mL^2\omega^2)\theta = -mL(R + L)\dot{\omega} \tag{3}$$

The term $(-mL^2\omega^2)$ indicates a reduction in the original stiffness of the system with increasing speed ω, so that for a spin speed greater than the natural frequency $k/(mL^2)$ of the system, angle θ will be unbounded. This is, of course, incorrect. The situation can be corrected as follows. Consider the additional potential energy of the "bar" BC due to geometric stiffness (see Ref. 20) caused by an axial force along the bar in the undeformed configuration of the system. The axial force in this case is the inertia force $m\omega^2(R + L)$, and the associated geometric stiffness gives rise to the potential energy

$$U_g = 0.5[w_1\ w_2]\frac{m\omega^2(R + L)}{L}\begin{bmatrix} 1 & -1 \\ -1 & 1 \end{bmatrix}\begin{Bmatrix} w_1 \\ w_2 \end{Bmatrix} \tag{4}$$

where w_1, w_2 are the transverse displacements at the end of the

bar. We set for the bar BC the boundary condition and small angle approximation, respectively,

$$w_1 = 0, \qquad w_2 = L\theta \tag{5}$$

Equations (4) and (5) together yield the potential energy due to the geometric stiffness of the bar

$$U_g = 0.5m\omega^2(R + L)L\theta^2 \tag{6}$$

The generalized active force associated with this additional potential energy is

$$F = -\frac{dU_g}{d\theta} = -m\omega^2(R + L)L\theta \tag{7}$$

Adding this to the right-hand side of Eq. (3) yields the correct equation that could be independently obtained with proper linearization without invoking the idea of geometric stiffness. This equation is

$$mL^2\ddot{\theta} + (k + m\omega^2RL)\theta = -mL(R + L)\dot{\omega} \tag{8}$$

Note that the term $(+m\omega^2RL)$ indicates an increase in stiffness over the original stiffness of the system for all ω, and this effect represents the phenomenon of dynamic stiffening. Figure 4 shows plots of two solutions—the solid one for Eq. (8) and the dashed one for Eq. (3)—for $R = L$ and the other parameters so chosen that the natural frequency $k/(mL^2)$ corresponds to 0.433 Hz, and ω is given by Eq. (1) with $\Omega = \pi$, $T = 30$. Note the qualitative similarity between Figs. 2 and 4. The solid curve in Fig. 2 represents dynamic stiffening of the paraboloidal antenna of Fig. 1, just as much as the solid curve of Fig. 4 represents dynamic stiffening for the system considered in this simple example. The dashed curves in Figs. 2 and 4 represent incorrect simulations. We will generalize the methodology used here for capturing dynamic stiffness in Secs. III and IV.

III. Generalized Inertia Forces

Here, we begin the development of dynamical equations for a single flexible body characterized by its vibration modes. Since the body is regarded as arbitrary, we are forced to linearize prematurely in the modal coordinates and their time derivatives. This error will be compensated for in Sec. IV. Consider the arbitrary flexible body of Fig. 5; its elastic motion, assumed "small," is referred with respect to a flying reference frame B attached to the flexible body at O and having "large" rigid-body rotations and translations in a Newtonian frame N. It is assumed that the flexible body is discretized as a system of "nodal" rigid bodies connected by springs in the finite-element sense. Let G be such a generic rigid body and G^* its mass center. Let the elastic displacement for G^* be given by

$$\delta = \sum_{j=1}^{\nu} \phi_j q_j \tag{9}$$

where ϕ_j is the space-dependent function representing the jth vibration mode and q_j the associated time-dependent function of modal coordinate for the body. Then, in terms of vector basis b_1, b_2, b_3 fixed in B, one can characterize the motion of G^* by first introducing the following generalized speeds (see Ref. 21, p. 40):

$$u_i = v^O \cdot b_i \qquad (i = 1,2,3) \tag{10}$$

$$u_{3+i} = \omega^B \cdot b_i \qquad (i = 1,2,3) \tag{11}$$

$$u_{6+i} = \dot{q}_i \qquad (i = 1,\ldots,\nu) \tag{12}$$

where v^O is the velocity of the point O in N, and ω^B the angular velocity of B in N. The velocity of G^* in N is then written as

$$v^G = \sum_{i=1}^{3} u_i b_i + \sum_{i=1}^{3} u_{3+i} b_i \times (r + \delta) + \sum_{i=1}^{\nu} \phi_j u_{6+j} \tag{13}$$

where r is the position vector from O to $\hat{G}^*$, the location of G^* in the undeformed configuration, and δ is the elastic displacement vector from $\hat{G}^*$ to G^*. The elastic rotation of G in B is again assumed to be small and given in terms of the jth modal rotation vector Θ_j by

$$\theta = \sum_{j=1}^{\nu} \Theta_j q_j \tag{14}$$

One can now write the angular velocity of G in N, invoking the addition theorem of angular velocities and using Eq. (12).

$$\omega^G = \sum_{i=1}^{3} u_{3+i} b_i + \sum_{i=1}^{\nu} \Theta_i u_{6+i} \tag{15}$$

Note that Eqs. (13) and (15) are already linear in the generalized speeds u_{6+i} $(i = 1,\ldots,\nu)$ associated with the modal coordinates, and this leads to error. However flawed as these equations are, they are the only ones available to an analyst wishing to describe the deformation of an arbitrary, general structure via modes. As mentioned before, we shall show how to compensate for this error presently. First, however, we note that the ith partial velocity of G^* in N and the ith partial angular velocity of G in N (see Ref. 21, pp. 45–50) associated with the generalized speeds u_i $(i = 1,\ldots,6 + \nu)$ can now be written by inspection and recorded as in Table 1.

Differentiation of the right-hand side of Eq. (13) with respect to t in N yields the acceleration of G^* in N

$$a^{G^*} = \sum_{j=1}^{3} [\dot{u}_j b_j + \dot{u}_{3+j} b_j \times (r + \delta)] + \sum_{j=1}^{\nu} \phi_j \dot{u}_{6+j} + \sum_{j=1}^{3} u_{3+j} b_j \times \left[\sum_{j=1}^{3} u_j b_j + \sum_{j=1}^{3} u_{3+j} b_j \times (r + \delta) + 2 \sum_{j=1}^{\nu} \phi_j u_{6+j} \right] \tag{16}$$

Similarly, the angular acceleration of G in N follows from Eq. (15).

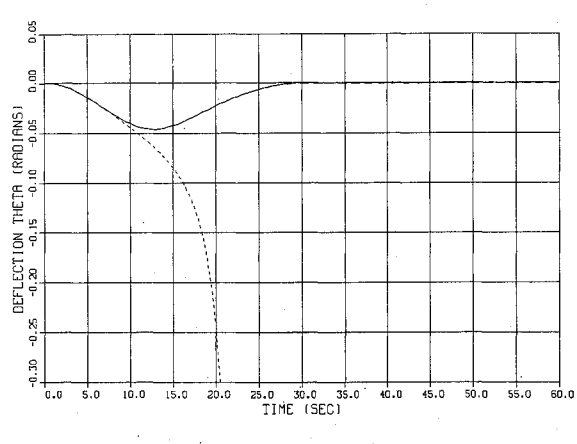

Fig. 4 Simulation results for system of Fig. 3, with dynamic stiffening (solid line) and without dynamic stiffening (dashed line).

Table 1 Partial velocities and partial angular velocities

i	$v_i^{G^*}$	ω_i^G
1, 2, 3	b_i	0
4, 5, 6	$b_i \times (r + \delta)$	b_i
7, 8,..., ν	ϕ_i	Θ_i

$$\alpha^G = \sum_{j=1}^{3}\left(\dot{u}_{3+j}b_j + u_{3+j}b_j \times \sum_{j=1}^{\nu}\Theta_j u_{6+j}\right) + \sum_{j=1}^{\nu}\Theta_j \dot{u}_{6+j} \quad (17)$$

The generalized inertia force (see Ref. 21, pp. 124-129) corresponding to the ith generalized speed is given by

$$F_i^* = -\int_D v_i^{G^*} \cdot a^{G^*}\, \mathrm{d}m - \int_D \omega_i^G \cdot \left[\tilde{\mathrm{d}}I^G \cdot \alpha^G + \omega^G \times \left(\tilde{\mathrm{d}}I^G \cdot \omega^G\right)\right] \qquad (i = 1,\ldots,6+\nu) \quad (18)$$

where $\mathrm{d}m$ and $\tilde{\mathrm{d}}I^G$ are the mass and central inertia dyadic for G, respectively, and the integrations are performed throughout the domain D occupied by the flexible body. With the partial velocities and partial angular velocities given by Table 1, the acceleration of G^* by Eq. (16), angular velocity and angular acceleration of G by Eqs. (15) and (17), respectively, the operations indicated in Eq. (18) become straightforward, although extremely tedious. What one must do is perform all the integrations over the spatial domain D in Eq. (18) in such a way that the integrands do not contain any time-varying quantities. The process of extracting time-invariant groups of terms from the integrands in Eq. (18) is performed by invoking certain vector-dyadic identities, and this yields all the modal integrals of Ho and Herber,[22] as well as some additional integrals due to the consideration of rotatory inertia in Eq. (18). The details of rewriting Eq. (18) in terms of the modal integrals are extensive, but not central to the issue at hand, and are not reported here for the sake of brevity. It is, however, important to note that Eq. (18) can be cast in the final form

$$-F_i^* = \sum_{j=1}^{6+\nu} M_{ij}\dot{u}_j + C_i \qquad (i = 1,\ldots,6+\nu) \quad (19)$$

where the elements of the time-dependent "mass matrix" M_{ij} $(i,j = 1,\ldots,6+\nu)$ are functions of the modal coordinates q_i $(i = 1,\ldots,\nu)$, and C_i $(i = 1,\ldots,6+\nu)$ are functions of the modal coordinates, as well as the generalized speeds u_i $(i = 1,\ldots,6+\nu)$.

IV. Generalized Active Forces

Here, we consider generalized active forces due to two kinds of internal forces. The first one is standard and is associated with structural stiffness, and the second one, associated here with motion stiffness, provides the mechanism of compensation for the aforementioned errors caused by premature linearization for an arbitrary flexible body undergoing the most general, large rotation and translation.

Generalized active forces due to structural elasticity are standardly written on the basis of mass-normalization of the vibration modes as

$$F_i^s = 0 \qquad (i = 1,\ldots,6)$$
$$= -\omega_{i-6}^2 q_{i-6} \qquad (i = 7,\ldots,6+\nu) \quad (20)$$

where ω_{i-6} and q_{i-6} are the $(i-6)$th vibration frequency and modal coordinate, respectively, $(i = 7,\ldots,6+\nu)$.

Motion stiffness, as we have conceived here, is a special case of geometric stiffness that is best treated in terms of finite-element theory. We recall (see Ref. 20) that geometric stiffness accounts for the effect of existing forces on bending stiffness, and that it depends only on the element's geometry, displacement field, and state of stress. Consider an element with existing stress components

$$\sigma_{xx0},\quad \sigma_{xy0},\quad \sigma_{xz0},\quad \sigma_{yy0},\quad \sigma_{yz0},\quad \sigma_{zz0}$$

and the $(3 \times n\text{DOF})$ matrix of interpolation functions $[N(x, y, z)]$, where nDOF stands for the element degrees of freedom, describing the displacement field as in

$$\{\delta\} = [N(x, y, z)]\{d\} \quad (21)$$

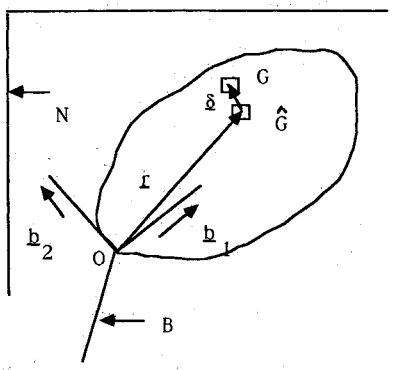

Fig. 5 Single flexible body with small elastic motion in a flying reference frame B having large rotation and translation in N.

where $\{\delta\}$ is a column matrix of three components of the elastic displacement at a point within the element and $\{d\}$ the column matrix of nDOF element nodal displacements. Then, the element geometric stiffness is derived from the strain energy stored as the existing stresses work through the strains representing the nonlinear parts of the Lagrangian strain components and is given by[20,23]

$$k_g^e = \int_e [N_{,x}^T\, N_{,y}^T\, N_{,z}^T] \begin{bmatrix} \sigma_{xx0}U_3 & \sigma_{xy0}U_3 & \sigma_{xz0}U_3 \\ \sigma_{xy0}U_3 & \sigma_{yy0}U_3 & \sigma_{yz0}U_3 \\ \sigma_{xz0}U_3 & \sigma_{yz0}U_3 & \sigma_{zz0}U_3 \end{bmatrix} \begin{Bmatrix} N_{,x} \\ N_{,y} \\ N_{,z} \end{Bmatrix} \mathrm{d}v \quad (22)$$

Here, a variable in the subscript preceded by a comma indicates differentiation with respect to that variable, and U_3 is the (3×3) unit matrix. In finite-element computer codes such as NASTRAN or EAL[24] (the latter used to generate the results reported in this paper), computation of geometric stiffness proceeds as follows: The distributed loading on the structure is first prescribed, and the corresponding linear static equilibrium problem is solved to determine the element stresses; then, element geometric stiffnesses are evaluated following Eq. (22), and the standard finite-element assembly procedure is used to construct the geometric stiffness matrix K_g for the whole structure. Now the following question arises: If geometric stiffness is to explain the phenomenon of dynamic stiffening, then what is the associated loading? The answer suggests itself: the loading brought into play by the motion itself, namely, the inertia forces and the inertia couples acting throughout the body. This is the reason for our choice of the label "motion stiffness."

We will now proceed to compute the motion stiffness of the structure due to these inertia loadings. The inertia force and couple on a generic, nodal rigid body G are considered, respectively, as follows:

$$f^* = -\mathrm{d}m a^{\hat{G}^*} \quad (23)$$

$$t^* = -\tilde{\mathrm{d}}I^{\hat{G}} \cdot \alpha^{\hat{G}} - \omega^{\hat{G}} \times (\tilde{\mathrm{d}}I^{\hat{G}} \cdot \omega^{\hat{G}}) \quad (24)$$

where $\hat{G}$ is the space occupied by G in the undeformed configuration of the structure (see Fig. 5), in analogy with the example of Sec. II. The acceleration of $\hat{G}^*$ in N is obtained by ignoring the terms involving elastic displacement in Eq. (16), which gives

$$a^{\hat{G}^*} = \sum_{j=1}^{3}\dot{u}_j b_j + \sum_{j=1}^{3}\dot{u}_{3+j}b_j \times r + \sum_{j=1}^{3}u_{3+j}b_j \times \left(\sum_{j=1}^{3}u_j b_j + \sum_{j=1}^{3}u_{3+j}b_j \times r\right) \quad (25)$$

We express r, the position vector of $\hat{G}^*$, and f^*, the inertia force on G in the undeformed configuration of the structure, in the vector basis fixed in the flying reference frame B as follows:

$$r = \sum_{j=1}^{3} x_j b_j \tag{26}$$

$$\begin{Bmatrix} t_1^* \\ t_2^* \\ t_3^* \end{Bmatrix} = -\begin{bmatrix} I_{11} & I_{12} & I_{13} & I_{13} & I_{33}-I_{22} & -I_{12} & 0 & I_{23} & 0 \\ I_{12} & I_{22} & I_{23} & -I_{23} & I_{12} & I_{11}-I_{33} & 0 & 0 & I_{13} \\ I_{13} & I_{23} & I_{33} & I_{22}-I_{11} & -I_{13} & I_{23} & I_{12} & 0 & 0 \end{bmatrix} \begin{Bmatrix} A_{13} \\ \vdots \\ A_{21} \end{Bmatrix} \tag{34}$$

$$f^* = \sum_{j=1}^{3} f_j^* b_j \tag{27}$$

Then, the inertia force on a typical point G of the structure, responsible for producing motion stiffness, may be seen as made up of the following 12 loadings [see Eqs. (23), (25-27)]:

$$\begin{Bmatrix} f_1^* \\ f_2^* \\ f_3^* \end{Bmatrix} = -\mathrm{d}m[U_3 \;\; x_1U_3 \;\; x_2U_3 \;\; x_3U_3] \begin{Bmatrix} A_1 \\ \vdots \\ A_{12} \end{Bmatrix} \tag{28}$$

where we have used for computational convenience the notations that follow. First, define

$$z_1 = u_5u_3 - u_6u_2 \tag{29a}$$

$$z_2 = u_6u_1 - u_4u_3 \tag{29b}$$

$$z_3 = u_4u_2 - u_5u_1 \tag{29c}$$

$$z_4 = u_4u_5 \tag{29d}$$

$$z_5 = u_6u_4 \tag{29e}$$

$$z_6 = u_5u_6 \tag{29f}$$

Then, $A_1,\ldots,A_{12}$ in Eq. (28) are given by

$$A_1 = \dot{u}_1 + z_1 \tag{30a}$$

$$A_2 = \dot{u}_2 + z_2 \tag{30b}$$

$$A_3 = \dot{u}_3 + z_3 \tag{30c}$$

$$A_4 = -(u_5^2 + u_6^2) \tag{30d}$$

$$A_5 = \dot{u}_6 + z_4 \tag{30e}$$

$$A_6 = -\dot{u}_5 + z_5 \tag{30f}$$

$$A_7 = -\dot{u}_6 + z_4 \tag{30g}$$

$$A_8 = -(u_6^2 + u_4^2) \tag{30h}$$

$$A_9 = \dot{u}_4 + z_6 \tag{30i}$$

$$A_{10} = \dot{u}_5 + z_5 \tag{30j}$$

$$A_{11} = -\dot{u}_4 + z_6 \tag{30k}$$

$$A_{12} = -(u_5^2 + u_4^2) \tag{30l}$$

Returning to the computation of the torque due to the inertia couple on G, we first obtain from Eqs. (15) and (17) the following:

$$\omega^{\hat{G}} = \sum_{j=1}^{3} u_{3+j} b_j \tag{31}$$

$$\alpha^{\hat{G}} = \sum_{j=1}^{3} \dot{u}_{3+j} b_j \tag{32}$$

Let t^* of Eq. (24) be expressed in the vector basis fixed in B as

$$t^* = \sum_{j=1}^{3} t_j^* b_j \tag{33}$$

Then, the inertia torque giving rise to geometric stiffness follows from Eqs. (24) and (31-33) and may be seen as made up of the following nine torque loadings:

where we have defined

$$A_{13} = \dot{u}_4 \tag{35a}$$

$$A_{14} = \dot{u}_5 \tag{35b}$$

$$A_{15} = \dot{u}_6 \tag{35c}$$

$$A_{16} = z_4 \tag{35d}$$

$$A_{17} = z_6 \tag{35e}$$

$$A_{18} = z_5 \tag{35f}$$

$$A_{19} = u_4^2 - u_5^2 \tag{35g}$$

$$A_{20} = u_5^2 - u_6^2 \tag{35h}$$

$$A_{21} = u_6^2 - u_4^2 \tag{35i}$$

With the force and torque loadings given by Eqs. (28) and (34), respectively, the finite-element code has to generate geometric stiffness matrices $K_g^{(i)}$ for unit values of each of the quantities $A_i (i = 1,\ldots,21)$, the multiplication by the actual values of these quantities being performed in the large motion dynamics code. Now, the generalized active forces due to this geometric stiffness and be derived in the same manner as those due to structural stiffness and are written as follows:

$$F_i^g = 0 \qquad (i = 1,\ldots,6) \tag{36}$$

$$\begin{Bmatrix} F_7^g \\ \cdot \\ F_{6+\nu}^g \end{Bmatrix} = -\sum_{i=1}^{21} S^{(i)} A_i q \tag{37}$$

Here, $S^{(i)}$ denotes the $(\nu \times \nu)$ generalized motion stiffness matrix corresponding to unit values of the ith inertia loading and is given by

$$S^{(i)} = \Phi^T K_g^{(i)} \Phi \tag{38}$$

where Φ is the modal matrix and q the $(\nu \times 1)$ matrix of modal coordinates. With expressions for the generalized inertia forces and generalized active forces now at hand, Kane's equations of motion (see Ref. 21, pp. 156-159) for the flexible body can be written as

$$\sum_{j=1}^{6+\nu} M_{ij}\dot{u}_j + C_i = 0 \qquad (i = 1,\ldots,6) \tag{39}$$

$$\begin{aligned} &\sum_{j=1}^{6+\nu} M_{i+6,j}\dot{u}_j + C_{i+6} + \omega_i^2 q_i \\ &+ \sum_{j=1}^{\nu} \Big\{ S_{ij}^{(1)}\dot{u}_1 + S_{ij}^{(2)}\dot{u}_2 + S_{ij}^{(3)}\dot{u}_3 + [S_{ij}^{(13)} - S_{ij}^{(9)} - S_{ij}^{(11)}]\dot{u}_4 \\ &\quad + [S_{ij}^{(14)} + S_{ij}^{(10)} - S_{ij}^{(6)}]\dot{u}_5 + [S_{ij}^{(16)} + S_{ij}^{(5)} - S_{ij}^{(7)}]\dot{u}_6 \\ &\quad + S_{ij}^{(1)}z_1 + S_{ij}^{(2)}z_2 + S_{ij}^{(3)}z_3 + [S_{ij}^{(5)} + S_{ij}^{(7)}]z_4 \\ &\quad + [S_{ij}^{(6)} + S_{ij}^{(10)}]z_5 + [S_{ij}^{(9)} + S_{ij}^{(11)}]z_6 \\ &\quad + S_{ij}^{(4)}A_4 + S_{ij}^{(8)}A_8 + S_{ij}^{(12)}A_{12} \\ &\quad + \sum_{k=16}^{21} S_{ij}^{(k)}A_k \Big\} q_j = 0 \qquad (i = 1,\ldots,\nu) \end{aligned} \tag{40}$$

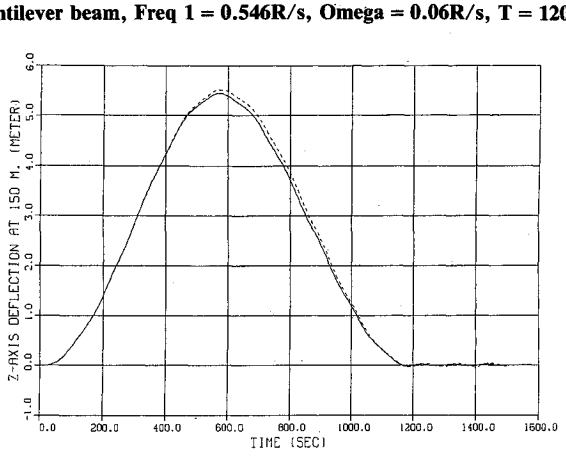

Fig. 6 Cantilever beam tip deflection during spin-up given by the present theory (solid line) and the theory of Ref. 1 for steady-state spin frequency greater than the first vibration mode frequency.

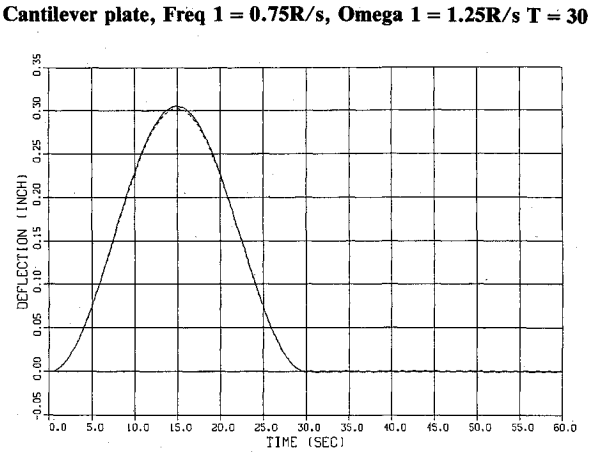

Fig. 7 Cantilever plate corner deflection during spin-up given by the present theory (solid line) and the theory of Ref. 3 for steady-state spin frequency greater than the first vibration mode frequency.

Note that when Eqs. (39) and (40) are written as the matrix differential equation

$$D\dot{U} = R \tag{41}$$

where U is the column matrix of the generalized speeds $(u_1,\ldots,u_{6+\nu})$, the coefficient matrix D becomes unsymmetric. Note also that in applications where rotatory inertia effects of a structure are insignificant, the second integral in Eq. (18) vanishes, and this simplifies Eq. (40) with

$$S_{ij}^{(k)} = 0 \qquad (k = 13,\ldots,21; \quad i,j = 1,\ldots,\nu) \tag{42}$$

In other words, only 12 and not 21 inertia stiffness matrices need to be computed if rotatory inertia is left out of account.

V. Algorithm

To implement the theory given in Secs. III and IV, the following step-by-step procedure must be used.

1) Using a code such as NASTRAN or EAL, construct the finite-element model of the structure with the origin of coordinates constrained to have zero degrees of freedom; generate the desired number ν of column matrices representing vibration modes and corresponding vibration frequencies.

2) On each node of the finite-element model, set up 12 forces defined by Eq. (28) with unit values of $A_1,\ldots,A_{12}$. If it is important to consider the rotatory inertia effects of the flexible body, then impose 9 torques as per Eq. (34) with unit values of $A_{13},\ldots,A_{21}$. This defines 12 or 21 sets of loads distributed throughout the body; next, for each set of loads compute the associated geometric stiffness matrix and convert the latter to the generalized motion stiffness matrix using Eq. (38).

3) Build a large motion dynamics code in which Eqs. (39) and (40) are developed. This involves the major work of construction of the M_{ij} and C_i terms of Eq. (19); next, the use of the generalized motion stiffness matrices as given in Eq. (40), along with the quantities $z_1,\ldots,z_6$ of Eq. (29) and A_4, A_8, A_{12}, $A_{16},\ldots,A_{21}$ of Eqs. (30) and (35), completes the assembly of the dynamical equation, Eq. (41).

4) Append standard kinematical equations (see Ref. 25, pp. 422–431) relating the time derivatives of the generalized coordinates defining the position of the origin and orientation of the flying reference frame B (see Sec. III) for the flexible body to the generalized speeds defined in Eqs. (10) and (11); kinematical equations for the modal coordinates are given by Eq. (12).

5) Assign initial values for the generalized speeds and generalized coordinates. If the initial deformations and deformation rates are given at a selected set of points, then the corresponding values for the modal coordinates and generalized speeds can be obtained by a pseudoinverse (see Ref. 25, pp. 312–313).

6) Integrate the dynamical and kinematical equations with these initial conditions.

VI. Validation

To validate the foregoing theory, which is applicable to an arbitrary flexible body, we compare motion predictions made by the new theory with known, correct predictions already in hand for beams[1] and plates.[3] In each case, correct prediction of structural deformations arising during the spin-up motion of the base of the structure in accordance with Eq. (1) is considered a crucial test of the validity of the present theory.

Figure 6 shows the transient behavior of tip deflection of a cantilever beam, relative to a line fixed in the rotating base and initially coincident with the axis of the undeformed beam, as given by the present theory (solid line) and the theory of Ref. 1 (dashed line), with rotatory inertia neglected in both cases. The beam is a 150-m-long antenna tube having a diameter of 0.0635 m and a wall thickness 0.00254 m, with the first bending frequency 0.0546 rad/s. In each of the two simulations, only the first four vibration modes of the beam are used. Spin-up of the base is described by Eq. (1), with a rise time $T = 1200$ s, and a steady-state spin frequency $\Omega = 0.06$ rad/s. The geometric stiffness used with the present theory for the EAL[24] beam element was dependent only on axial force and did not include the effects of transverse shear, and this may explain the slight discrepancy between the two curves in Fig. 6. The overall agreement between the two curves in Fig. 6 furnishes evidence of the adequacy with which the present theory reproduces dynamic stiffening.

Results of comparing the present theory with that of Ref. 3, for a cantilever plate being spun up about an edge, are shown in Fig. 7. The plate is 72 in. long, 48 in. wide, and 0.1 in. thick, and has a first natural frequency of 0.75 rad/s. Again, the spin-up is described by Eq. (1), with $T = 30$ s and $\Omega = 1.25$ rad/s. In this case, the first six vibration modes of the plate are used in each simulation, and the difference between the results on corner deflection of the plate in Fig. 7 between the present theory (solid curve) and theory of Ref. 3 (dashed curve) is hardly discernible. When one recalls that the theories in Refs. 1 and 3 capture dynamic stiffening by linearizing correctly in consistency with the deformation constraints that are applicable only to beams and plates, the reproduction of these results with a general-purpose theory valid for any arbitrary structure must be deemed most gratifying.

VII. Conclusions

We have presented a general theory for capturing dynamic stiffening of an arbitrary flexible body undergoing large rotation and translation accompanied by small vibrations. The theory identifies such motion-induced stiffness as geometric stiffness due to a system of 12 inertia forces and 9 inertia couples distributed throughout the body. This geometric stiffness is preprocessed by a standard finite-element code and does not render the simulation computationally intensive. Consistent with the small elastic displacement assumption, the formulation provides a first-order representation of the geometric stiffness, and not the additional stiffness that may be obtained from a consideration of the dynamic elastic deformation of the structure. Numerical results show that the theory presented here for an arbitrary structure reproduces the results predicted by special-purpose theories of dynamic stiffening of beams and plates. In conclusion, it may be seen that the theory is sufficiently general and it provides a basis for correcting software packages that fail to represent dynamic stiffening, without requiring extensive additional computations.

Acknowledgment

Arun Banerjee would like to dedicate this paper to Prof. Thomas R. Kane as a token of appreciation for many enlightening discussions over the years on the subject of dynamics.

References

[1]Kane, T. R., Ryan, R. R., and Banerjee, A. K., "Dynamics of a Cantilever Beam Attached to a Moving Base," *Journal of Guidance, Control, and Dynamics,* Vol. 10, March-April 1987, pp. 139-151.

[2]Man, G. and Laskin, R., (eds.), *Proceedings of the Workshop on Multibody Simulation,* NASA Jet Propulsion Lab., California Inst. of Technology, Pasadena, CA, April 15, 1988.

[3]Banerjee, A. K. and Kane, T. R., "Dynamics of a Plate in Large Overall Motion," *Journal of Applied Mechanics,* Vol. 56, Dec. 1989, pp. 887-892.

[4]Bisplinghoff, R. L., Ashley, H., and Halfman, R. L., *Aeroelasticity,* Addison-Wesley, Reading, MA, 1955, pp. 95-97.

[5]Meirovitch, L., *Analytical Methods in Vibrations,* MacMillan, New York, pp. 443-445.

[6]Likins, P. W., "Geometric Stiffness Characteristics of a Rotating Elastic Appendage," *International Journal of Solids and Structures,* Vol. 10, No. 2, 1974, pp. 161-167.

[7]Levinson, D. A. and Kane, T. R., "Spin Stability of a Satellite Equipped with Four Booms," *Journal of Spacecraft and Rockets,* Vol. 13, April 1976, pp. 208-213.

[8]Turcic, D. A. and Midha, A., "Generalized Equations of Motion for the Dynamic Analysis of Elastic Mechanism Systems," *ASME Journal of Dynamic Systems, Measurement, and Control,* Vol. 106, Dec. 1984, pp. 243-248.

[9]Turcic, D. A., Midha, A., and Bosnik, J. R., "Dynamic Analysis of Elastic Mechanism Systems. Parts I & II," *ASME Journal of Dynamic Systems, Measurement, and Control,* Vol. 106, Dec. 1984, pp. 249-260.

[10]Simo, J. C. and Vu-Quoc, L., "On the Dynamics of Flexible Bodies Under Large Overall Motions—The Plane Case: Parts I & II," *Journal of Applied Mechanics,* Vol. 53, Dec. 1986, pp. 849-863.

[11]Vu-Quoc, L. and Simo, J. C., "Dynamics of Earth-Orbiting Satellites with Multibody Components," *Journal of Guidance, Control, and Dynamics,* Vol. 10, Nov. 1987, pp. 549-558.

[12]Housner, J., McGowan, P. E., Abrahamson, L. A., and Powell, M. G., "LATDYN User's Manual," NASA TM-87635, Jan. 1986.

[13]Wu, S.-C. and Haug, E. J., "Geometric Nonlinear Substructuring for Dynamics of Flexible Mechanical Systems," *International Journal for Numerical Methods in Engineering,* Vol. 26, No. 10, 1988, pp. 2211-2221.

[14]Hopkins, A. S. and Likins, P. W., "Analysis of Structures with Rotating, Flexible Substructures," *Proceedings of the AIAA/ASME/ASCE/AHS 28th Structures, Structural Dynamics and Materials Conference,* AIAA, New York, 1987, pp. 944-954.

[15]Modi, V. J. and Ibrahim, A. M., "On the Dynamics of Flexible Orbiting Structures," *Large Space Structures: Dynamics and Control,* edited by S. N. Atluti and A. K. Amos, Springer-Verlag, New York, 1988, pp. 93-114.

[16]Zeiler, T. and Buttrill, C., "Dynamic Analysis of an Unrestrained Rotating Structure Through Nonlinear Simulation," *Proceedings of the AIAA/ASME/ASCE/AHS 27th Structures, Structural Dynamics and Materials Conference,* AIAA, Washington, DC, April 1988, pp. 167-174.

[17]Amirouche, F. M. L. and Ider, S. K., "The Influence of Geometric Nonlinearities in the Dynamics of Flexible Tree-Like Structures," *Journal of Guidance, Control, and Dynamics,* Vol. 12, No. 6, 1989, pp. 830-837.

[18]Bodley, C. S., Devers, A. D., Park, A. C., and Frisch, H. P., "A Digital Computer Program for the Dynamic Interaction Simulation of Controls and Structures (DISCOS)," Vols. I & II, NASA TP-1219, May 1978.

[19]Singh, R. P., van der Voort, R. J., and Likins, P. W., "Dynamics of Flexible Bodies in Tree Topology—A Computer Oriented Approach," *Journal of Guidance, Control, and Dynamics,* Vol. 8, Sept.-Oct. 1985, pp. 584-590.

[20]Cook, R. D., *Concepts and Applications of Finite Element Analysis,* McGraw-Hill, New York, 1985, pp. 331-341.

[21]Kane, T. R. and Levinson, D. A., *Dynamics: Theory and Applications,* McGraw-Hill, New York, 1985.

[22]Ho, J. Y. L. and Herber, D. R., "Development of Dynamics and Control Simulation of Large Flexible Space Systems," *Journal of Guidance, Control, and Dynamics,* Vol. 8, May-June 1985, pp. 374-383.

[23]Zienkeiwicz, O. C., *The Finite Element Method,* McGraw-Hill, New York, 1977, pp. 517-519.

[24]Whetstone, W. D., "EISI-EAL Engineering Analysis Language Reference Manual," Engineering Information Systems, Inc., San Jose, CA, July 1983.

[25]Kane, T. R., Likins, P. W., and Levinson, D. A., *Spacecraft Dynamics,* McGraw-Hill, New York, 1983.